An extended "perfect-plasticity" method for estimating ice thickness along the flow line of mountain glaciers

Huilin Li,[1] Felix Ng,[2] Zhongqin Li,[1,3] Dahe Qin,[1] and Guodong Cheng[1]

Received 26 May 2011; revised 3 December 2011; accepted 6 December 2011; published 29 February 2012.

[1] Direct measurement of the thickness of mountain glaciers is difficult over large areas, yet knowledge of the thickness is essential for calculating their volumes and future evolution. We develop a new method for estimating the ice thickness along glacier flow lines, using the "perfect-plasticity" rheological assumption that relates the thickness and surface slope to a yield stress. Previous studies have used this assumption with the shallow-ice approximation to estimate the ice thickness, but the standard approach neglects the effect of side drag on glacier stress balance. Our method addresses this shortcoming and extends the standard method by accounting for the side drag via the glacier width. Besides the assumed yield stress, the inputs for our method are the outline and surface topography of the glacier; surface velocity and mass balance data are unnecessary. We validated the extended method on five glaciers in northwest China where thickness data are available from radio echo soundings, finding that it can reproduce measured thicknesses with a mean absolute error of 11.8% (like the standard method). Moreover, for long glacier tongues confined to flow between parallel valley sides, this method is found to give more accurate thickness estimates than does the standard method, with a mean absolute error of as low as 5.3%. Sensitivity analysis shows that the estimated ice thickness depends strongly on yield stress and surface slope and less strongly on glacier width. Because this method is physically more realistic than the standard method and its inputs are easily derivable from remote-sensing observations, it has the potential to be used for processing large glacier data sets.

Citation: Li, H., F. Ng, Z. Li, D. Qin, and G. Cheng (2012), An extended "perfect-plasticity" method for estimating ice thickness along the flow line of mountain glaciers, *J. Geophys. Res.*, *117*, F01020, doi:10.1029/2011JF002104.

1. Introduction

[2] Glaciers in many regions of the world are retreating under sustained negative mass balances that have been linked to climatic warming [see *Lemke et al.*, 2007]. This has raised concerns for the consequential impact on downstream human settlements and ecosystems. In particular, the need for reliable projection of future meltwater availability [e.g., *Kaser et al.*, 2010] and sea level rise [e.g., *Raper and Braithwaite*, 2006] provides a strong motivation for estimating glacier volumes. Determination of the thickness of glaciers is crucial in this context. While the spatial distribution of ice thickness on a glacier converts straightforwardly into a volume estimate, the thickness is also a factor behind the driving stress of glacier motion, and hence behind the glacier's response to climate change. Indeed, knowledge of present-day ice thickness is typically needed for defining the initial glacier geometry in models that simulate glacier flow and runoff into the future [e.g., *Aðalgeirsdóttir et al.*, 2006; *Björnsson et al.*, 2006; *Hubbard et al.*, 1998; *Huss et al.*, 2008; *Huybrechts and de Wolde*, 1999; *Oerlemans et al.*, 1998].

[3] Radio echo sounding and borehole drilling can yield reliable point measurements of the ice thickness, but these field techniques are impractical when the glaciers concerned are remote or numerous [*Farinotti et al.*, 2009]. Alternative approaches of estimating the thickness have therefore been developed, often with the aim to treat large samples of glaciers and capitalize on readily available (e.g., remote sensing) data on ice-surface parameters. One method uses volume-area scaling relations for glaciers [*Bahr et al.*, 1997; *Chen and Ohmura*, 1990; *Driedger and Kennard*, 1986; *Van de Wal and Wild*, 2001; *Radic and Hock*, 2010], although the validity of applying this to individual glaciers has been questioned [*Arendt et al.*, 2006]. Other methods involve viscous flow mechanics of the ice explicitly. For instance, rigorous inversions [*Raymond and Gudmundsson*, 2009; *Thorsteinsson et al.*, 2003] have been developed for ice streams that enable inference of their basal properties, including their bed elevation. Such methods require a known surface velocity field as input. For alpine glaciers, *Farinotti et al.* [2009] recently described a method of estimating their

[1]State Key Laboratory of Cryospheric Sciences, Tian Shan Glaciological Station, CAREERI, CAS, Lanzhou, China.
[2]Department of Geography, University of Sheffield, Sheffield, UK.
[3]College of Geography and Environment Sciences, Northwest Normal University, Lanzhou, China.

0148-0227/12/2011JF002104

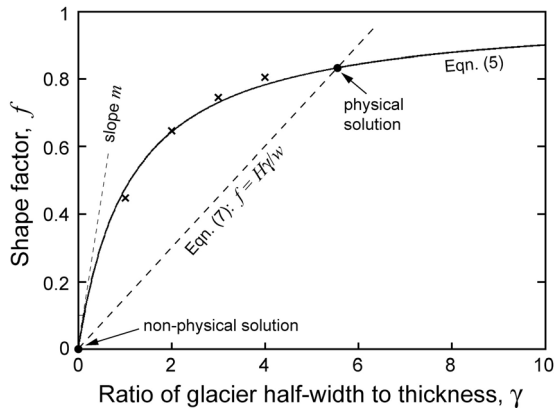

Figure 1. The function $f(\gamma)$ used to approximate the values of shape factor listed in Table 1 (crosses).

thickness that combines glacier mass turnover with viscous flow mechanics. The input of this method is mass balance rather than velocity observations, but such data are still difficult to acquire for large samples of glaciers. Yet another class of methods employs the perfect-plasticity assumption [*Nye*, 1951] instead of the viscous assumption for ice rheology to estimate the thickness. They have been popular for reconstructing the paleo surface profiles of ice sheets [e.g., *Beget*, 1987; *Paterson*, 1994; *Reeh*, 1982, 1984] and glaciers [*Schilling and Hollin*, 1981; *Benn and Hulton*, 2010; *Ng et al.*, 2010] from landform evidence. They have also been applied to modern glaciers for estimating their thickness [*Driedger and Kennard*, 1986; *Gerrard et al.*, 1952; *Haeberli and Hoelzle*, 1995; *Huybrechts et al.*, 1989; *Oerlemans*, 1997; *Paul and Svoboda*, 2010], usually with the effect of valley side drag ignored or treated as constant. Finally, *Clarke et al.* [2009] explored a disparate method of estimating the ice thickness in ice-covered terrain, based on training artificial neural networks to simulate subglacial topography that is geometrically similar to neighboring ice-free topography. They found promise for this method for yielding reasonable regional ice-volume estimates, despite considerable errors in its local estimates of the ice thickness.

[4] Here we propose a new way of estimating the ice thickness along glacier flow lines based on the perfect-plasticity assumption. In section 2.1 we first outline this assumption, which leads to a relationship between ice thickness, surface slope and an assumed (plastic) yield stress. In the standard method of estimating the thickness, the user inputs data of surface slope and yield stress into the relationship to find the thickness without accounting for other factors. In section 2.2 we then explain our extended method, which incorporates glacier width into the description. This method innovatively combines the "shape factor" representing the influence of side drag on the stress balance [*Paterson,* 1994, pp. 267–269] with the standard method, a realistic extension that recognizes explicitly the width-to-depth ratio of the glacier. Our method thus fills a gap in the range of existing methods. In sections 3 and 4, we apply it to five mountain glaciers in northwest China (Figure 1) and compare its performance to that of the standard method. Section 5 presents our conclusions and outlook. The paper by *Farinotti et al.* [2009] set a good example of how to report and evaluate new methods of glacier thickness estimation. We therefore follow their style of presentation in this paper, even though our method and its physical basis and results are completely different from theirs.

2. Theory

2.1. Standard Method

[5] *Paterson* [1970a, 1970b], building upon *Nye*'s [1952] theory for the flow mechanics of an infinitely wide glacier, suggested that the ice thickness h can be found from the ice surface slope α by the relation

$$h = \frac{\tau_b}{\rho g \sin\alpha}, \tag{1}$$

where ρ is ice density, g is gravitational acceleration, and τ_b is basal shear stress. The quantity τ_b is equated to a constant yield stress τ_y under the perfect-plasticity assumption for the flow rheology [*Nye*, 1951]. Equation (1) describes stress balance under the shallow-ice approximation, with longitudinal stress gradients ignored.

2.2. Extended Method

[6] We modify the standard method to account for the width of the glacier cross section (assumed symmetrical). *Nye* [1965] computed numerical solutions for the steady rectilinear flow of ice, obeying Glen's nonlinear flow law with $n = 3$, down uniform cylindrical channels of rectangular, semielliptic and parabolic cross sections. According to his analysis, since the valley walls support part of the glacier's weight, the basal shear stress on the centerline is less than that for an infinitely wide channel and may be found from

$$\tau_b = f \rho g h \sin\alpha, \tag{2}$$

where h refers to the ice thickness on the centerline and $f (\leq 1)$ is a shape factor that depends on the aspect ratio of the cross section, specifically, on the ratio of its half width w to the thickness,

$$\gamma = \frac{w}{h}. \tag{3}$$

The concept of the shape factor f was first introduced by *Nye* [1965], and Table 1 lists his values of f for a parabolic section.

[7] Given data for the half width w, the surface slope α, basal shear stress τ_b (= τ_y), and the function $f(\gamma)$, equations (2) and (3) may be solved for h simultaneously. This is the idea behind our extended method. In particular,

Table 1. Shape Factor f for Glacier Flow Through Parabolic Cross Sections With Different Values of γ, Where γ Is the Ratio of the Half Width of the Cross Section to Its Centerline Thickness[a]

$\gamma = w/h$	f
0	0
1	0.445
2	0.646
3	0.746
4	0.806
∞	1.000

[a]The data here originate from *Nye* [1965, Table 4]. Nye used the symbol W in place of γ.

since the shape factor depends on h, the problem is algebraic. As far as our literature search shows, previous researchers (including Nye) have not solved equations (2) and (3) in this way for estimating the ice thickness within the perfect-plasticity context, although these equations have often been used for forward evaluation of the basal shear stress. It is noteworthy also that *Schilling and Hollin* [1981] used the same ingredients to find the thickness h of paleoglaciers, but their problem differs conceptually and mathematically from ours because it is the former surfaces (not beds) of paleoglaciers that require reconstruction. Since α is thus unknown, their method involves integrating equation (2) as a first-order differential equation for h, given data for the glacier-bed profile [e.g., see *Benn and Hulton*, 2010].

[8] Glacial valley cross sections are often described as U-shaped [*Harbor*, 1990; *Harbor and Wheeler*, 1992; *Hirano and Aniya*, 1988]. To model this shape, *Svensson* [1959] introduced the power law

$$Y = aX^b, \tag{4}$$

where X and Y are horizontal and vertical distances from the lowest point of the cross profile, respectively, and a and b are constants quantifying the profile's aspect ratio and curvature. Equation (4) is commonly used in morphometric analyses of glacial troughs, which show that b ranges from less than 1 to over 5, with most values falling between 1.5 to 2.5, near the parabola value, $b = 2.0$ [*Aniya and Welch*, 1981; *Doornkamp and King*, 1971; *Graf*, 1970; *Li et al.*, 2001]. Using variation principle, *Hirano and Aniya* [1988] showed that a model of glacier erosion that minimizes friction between ice and bed also produces cross-sectional profiles with $b = 2.0$.

[9] In the present study, we assume a parabolic cross section and hence the values of f in Table 1, and we represent these values by the function

$$f(\gamma) = 1 - \frac{1}{1 + m\gamma} \tag{5}$$

with $m = 0.9$, which fits them well ($R^2 = 0.999$); see Figure 1. Although real glacier cross sections are not exactly parabolic and symmetric, this extension already improves upon equation (1), which neglects glacier width altogether. For comparison, values of $f(\gamma)$ supplied by *Nye* [1965] for elliptic and rectangular flow cross sections differ from those in Table 1 by 9% on average. Another way of deriving a shape factor, $f = A_c/(hP)$ [*Budd*, 1969, p. 45], where A_c is the cross section's area and P its perimeter on the ice-bed interface, gives values of f different from those in Table 1 by 10% on average.

[10] Now, substituting f from equation (5) into equation (2) with $\gamma = w/h$ taken from equation (3) and with the basal shear stress set at the yield stress, and solving for the centerline ice thickness, gives

$$h = \frac{mwH}{mw - H} = \frac{H}{1 - \frac{H}{mw}}, \tag{6}$$

where we take $m = 0.9$ and where $H = \tau_y/(\rho g \sin\alpha)$ is the thickness predicted by the standard method. Equation (6) is our extended method. With w being finite, the denominator $(1 - H/mw) < 1$ and we find $h > H$, which is expected because some of the driving stress $\rho g h \sin\alpha$ is supported by lateral drag, not all of it by the yield stress at the bed. At the limit $w \to \infty$ we recover the result of the standard method: $h = H$.

[11] We can understand other mathematical properties of the extended method by eliminating h between equations (2) and (3) to give

$$f = \frac{H}{w}\gamma, \tag{7}$$

and by seeing on Figure 1 where this straight line intersects $f(\gamma)$. This construction shows two solutions of the problem of solving equations (2), (3), and (5) for h. The intersection at $\gamma = f = 0$ (which corresponds to $h \to \infty$) identifies a nonphysical solution. The other intersection identifies the physical solution in equation (6). Figure 1 shows that if the glacier width is so small that $H/w > m$, then the latter solution ceases to exist because equation (7) is a steep line that no longer intersects $f(\gamma)$ in $\gamma > 0$; then equation (6) gives a negative ice-thickness estimate. This problem could be overcome by designing a different form for $f(\gamma)$ with infinite slope at $\gamma = 0$, but tempering this local behavior does not concern us here because we expect real glaciers to be thin, with $\gamma > 1$. On the other hand, flat regions on glaciers could have small slopes α that make H large, causing $H/w > m$. When using equation (6), we therefore impose a slope limit α_0 and set any lower observed slope α to it. Such filtering has been used elsewhere [e.g., *Farinotti et al.*, 2009].

2.3. Implementation

[12] Given a glacier with known outline and surface topography, we use equation (6) to estimate the glacier centerline thickness for various cross sections along its length, and then we find its total volume from an interpolated map of the thickness. We derive inputs to equation (6) as follows. First, a central flow line for the glacier is traced by linking the points of maximum curvature on its surface contours (F. Paul et al., Guidelines for the compilation of glacier inventory data from digital sources, World Glacier Monitoring Services, 2010, http://globglacier.ch/docs/guidelines_inventory.pdf). At each point of interest on the flow line, a perpendicular line drawn (in plan view) to the glacier edges defines the "full width" (FW) of the cross section. We take half of this width as w, and take α from the surface slope of the flow line evaluated at the point, subject to the minimum limit α_0 described above. To ensure consistency with the shallow-ice approximation, α should be evaluated from surface topographic data as the average slope over a horizontal distance that is several times of the local ice thickness [*Kamb and Echelmeyer*, 1986]. Since the ice thickness is not known a priori, iteration is generally needed to find a suitable averaging distance. For the glaciers studied by us in sections 3 and 4, we used an averaging distance of 400 m, which turns out to be 8 to 12 times of their mean ice thickness.

[13] For each cross section, we define also an "effective width" (EW), based on that stretch of the ice surface whose slope (in the section) does not exceed a threshold slope, α_{lim} [see *Farinotti et al.*, 2009]. This threshold helps to exclude snow and ice on valley sides not contributing to the stress balance.

[14] Note that cross sections envisaged in our extended method are idealized compared to their real geometries,

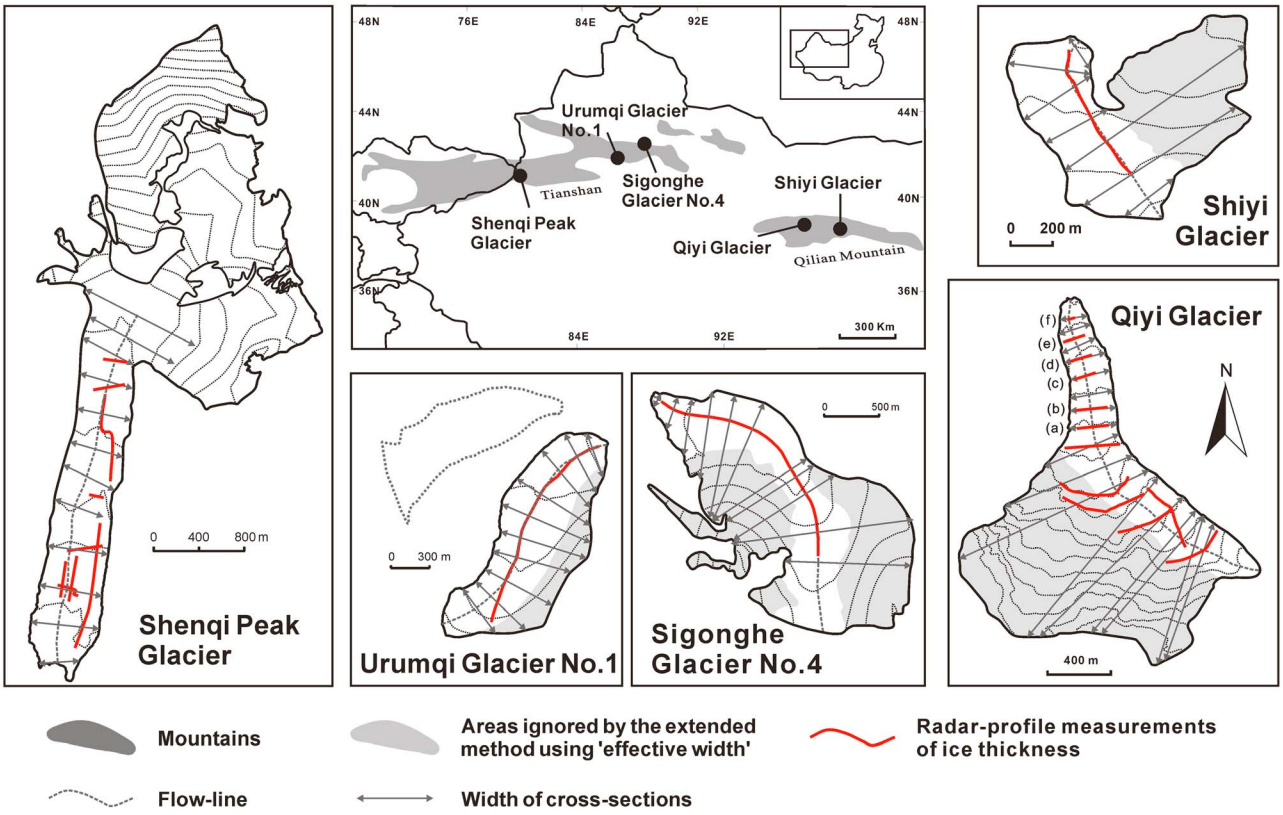

Figure 2. Topography of the glaciers used in our study. The top center map locates them in China. Contour intervals for surface elevation are 100 m. Red curves indicate profiles of radar measurements of ice thickness. Double-headed arrows indicate the full width of cross sections. Grey shading shows areas excluded from the effective width of cross sections. The map of Urumqi Glacier No. 1 shows the topography of its east branch and only outlines its west branch. Points a–f in the map for Qiyi Glacier identify the cross sections in Figure 5.

which are likely to be nonparabolic and have asymmetric bed and surface profiles. The flow line itself may be offset from the midpoint of the cross section. Also we neglect the potential impact of basal sliding on the shape factor f, whose values in Table 1 assume no slip (the boundary condition used by *Nye* [1965]).

[15] In section 3, we present and compare estimates of glacier thickness found with the standard method (SM) and extended method (EM). For the latter, calculations are made with w taken separately as half of the full width (FW) and half of the effective width (EW). Thus three methods are considered in all. We label them with the abbreviations SM, EM-FW, and EM-EW for ease of discussion.

3. Application and Results

3.1. Glacier Data

[16] According to *Shi et al.* [2006, 2008a, 2008b], glaciers in the Tian Shan and Qilian Shan in northwest China constitute 46.8% of the total number (46,400) of glaciers in China; they tend to be continental or "cold" glaciers and are relatively small in size, with a mean area of 1.3 km^2. These glaciers provide a vital water source for 130 million people and the regional ecosystem, but, under recent climatic warming, have been shrinking rapidly [*Li et al.*, 2010]. This context makes them suitable candidates for a first application of our method.

[17] Five glaciers from this region are used in the present study, three from the Tian Shan (Shenqi Peak Glacier, the east branch of Urumqi Glacier No. 1, Sigonghe Glacier No. 4) and two from Qilian Shan (Qiyi Glacier, Shiyi Glacier). Figure 2 shows their location and topography, and Table 2 lists key data for them. Situated in mountainous terrain, all five are valley glaciers thought to contain subtemperate ice. Observed surface velocities on Urumqi Glacier No. 1 and Shenqi Peak Glacier indicate they are predominantly cold-based, with basal sliding occurring only close to their snouts and in summer [*Zhou et al.*, 2009; *Cao et al.*, 2011]. Shiyi Glacier flows north and splits into two branches owing to the presence of a bedrock obstacle.

[18] We chose these glaciers because radio echo soundings have been carried out on them to measure the ice thickness (typically every 4 or 10 m along profiles). These thickness measurements have been published for Urumqi Glacier No. 1 [*Wang et al.*, 2011] and Sigonghe Glacier No. 4 [*Wu et al.*, 2011]; the radar-measured thicknesses for the other three glaciers are presented here for the first time. The radar profiles on Urumqi Glacier No. 1, Shiyi, and Sigonghe Glacier No. 4 lie on the defined central flow lines and cover much of their lengths, and the corresponding measured

Table 2. Data for the Five Glaciers Used in Our Study[a]

Glacier	Latitude (°N), Longitude (°E)	Area (km^2)	Approximate Length (km)	Number of Radar Profiles	Year of Radar Profiling	Year of DEM	ELA (m) and Period of Its Determination
Shiyi	38°12′48″, 99°52′40″	0.68	1.0	1	2010	2010	4440, Sep 2008 to Aug 2009
Qiyi	39°14′15″, 97°45′23″	2.98	3.8	12	1980	1975	4970, Sep 2001 to Aug 2003
Sigonghe Glacier No. 4	43°50′03″, 88°19′34″	2.80	3.1	1	2009	2009	3950, Sep 2008 to Aug 2009
Urumqi Glacier No. 1 (east branch)	43°06′51″, 86°48′39″	1.09	2.0	1	2006	2006	4000, Sep 2001 to Aug 2008
Shenqi Peak	41°46′08″, 79°53′19″	5.64	6.0	6	2008	2008	4850, Sep 2007 to Aug 2009

[a]DEM refers to digital elevation model of glacier surface topography, and ELA refers to glacier equilibrium line altitude. In the ELA column, each ELA derives from stake measurements of glacier mass balance and is an average value determined for the period given.

thicknesses will be compared directly with our thickness estimates below. The radar profiles on Shenqi Peak and Qiyi, two glaciers with well-defined lower tongues, are concentrated on these tongues. As only several short profiles on Shenqi Peak lie on the flow line and most profiles on Qiyi are transverse, giving relatively few measurements on the flow lines, we interpolate these measurements (by inverse distance averaging) to generate "measured thicknesses" for the comparisons.

[19] The outlines and digital elevation models (DEMs) of all five glaciers are also known for the years listed in Table 2. For Qiyi Glacier, these data derive from a 1:12,000-scale topographic map with a vertical accuracy of ±10 m. For Urumqi Glacier No. 1, these data were obtained by ground survey using a digital theodolite with a laser distance meter; elevation errors are estimated to be ±0.1 m after accounting for the instruments' settings and the network of theodolite benchmarks. The data for the other glaciers (Shiyi, Sigonghe Glacier No. 4, and Shenqi Peak) were obtained also by ground survey, but with a differential Global Positioning System that has positional accuracy of the order of centimeters.

3.2. Optimal Thickness Estimates

[20] To investigate how well the three methods (SM, EM-FW, EM-EW) work, we follow the procedure of deriving ice-thickness estimates along the flow line of each glacier as described in section 2.3, and compare these estimates with the radar-measured thicknesses. Each method is applied to each of the five glaciers. In each application, we quantify the overall mismatch by the mean absolute error between the estimated and measured thicknesses, here termed "average deviation."

[21] In this validation exercise, no preconceived universal value of the yield stress is used because the basal resistance encapsulated by τ_y involves many factors (e.g., ice viscosity, basal sliding, subglacial deformation) that may cause τ_y to vary much across different glaciers and make its estimation highly uncertain [see *Paterson*, 1994]. Instead, in each application we assume τ_y to be constant for each glacier, and calibrate its value to obtain the best thickness match by minimizing the average deviation. Accordingly, we will not test each method generally by seeing how accurately it can predict the ice thickness without prior information on τ_y for each glacier. However, we test each method by assessing how well it reproduces along-flow variations in the thickness after τ_y has been calibrated. (A method that fails this test clearly does not work.) This choice avoids circularity between testing and calibration. We leave the more general test to future work that analyses data sets containing many more glaciers.

[22] In the validation, the two slope parameters in the extended methods (the limit α_0 and the threshold $\alpha_{\lim}$) are assumed constant for all glaciers and calibrated alongside τ_y in the following way. First, with each combination of α_0 and $\alpha_{\lim}$ within the ranges $0° < \alpha_0 < 10°$ and $0° < \alpha_{\lim} < 60°$ (and both of these angles stepping in increments of 1°), the optimal τ_y and the associated average deviations are computed for all 15 applications (three methods, five glaciers), and we note the lowest average deviation among these. We then seek the combination of α_0 and $\alpha_{\lim}$ that minimizes the lowest average deviation. The final results are $\alpha_0 = 4°$ and $\alpha_{\lim} = 30°$, and Table 3 lists the corresponding values of τ_y.

[23] With these optimal parameters, the three methods have been applied to each glacier to estimate its flow line thickness, and Figure 3 plots the corresponding bed profiles found by subtracting the thickness from the glacier surface. The bed elevations determined by radar measurements are also shown. The estimated bed profiles fit the measured ones reasonably well, often capturing thickness variations down to a horizontal distance scale of a few hundred meters. Shenqi Peak Glacier has identical EM-FW and EM-EW results because cross sections on its tongue (where the radar profiles are located) have nearly flat surfaces, making their effective widths equal to their full widths.

[24] Figure 4 compares the estimated and measured ice thicknesses on scatterplots, showing good correlations for all three methods. Thickness estimates in the standard method explain 88% of the variance in the measured thicknesses of all five glaciers; the corresponding numbers in the extended methods are 88.2% (EM-FW) and 86.8% (EM-EW). All

Table 3. Optimal Values of the Yield Stress τ_y (kPa) When Using Each Thickness-Estimation Method on Each Glacier[a]

Method	Shenqi Peak Glacier	Urumqi Glacier No. 1 (East Branch)	Sigonghe Glacier No. 4	Qiyi Glacier	Shiyi Glacier
SM	74	154	83	175	96
EM-FW	50	114	69	125	77
EM-EW	50	105	56	110	73

[a]SM, standard method; EM-FW, extended method using full width; EM-EW, extended method using effective width.

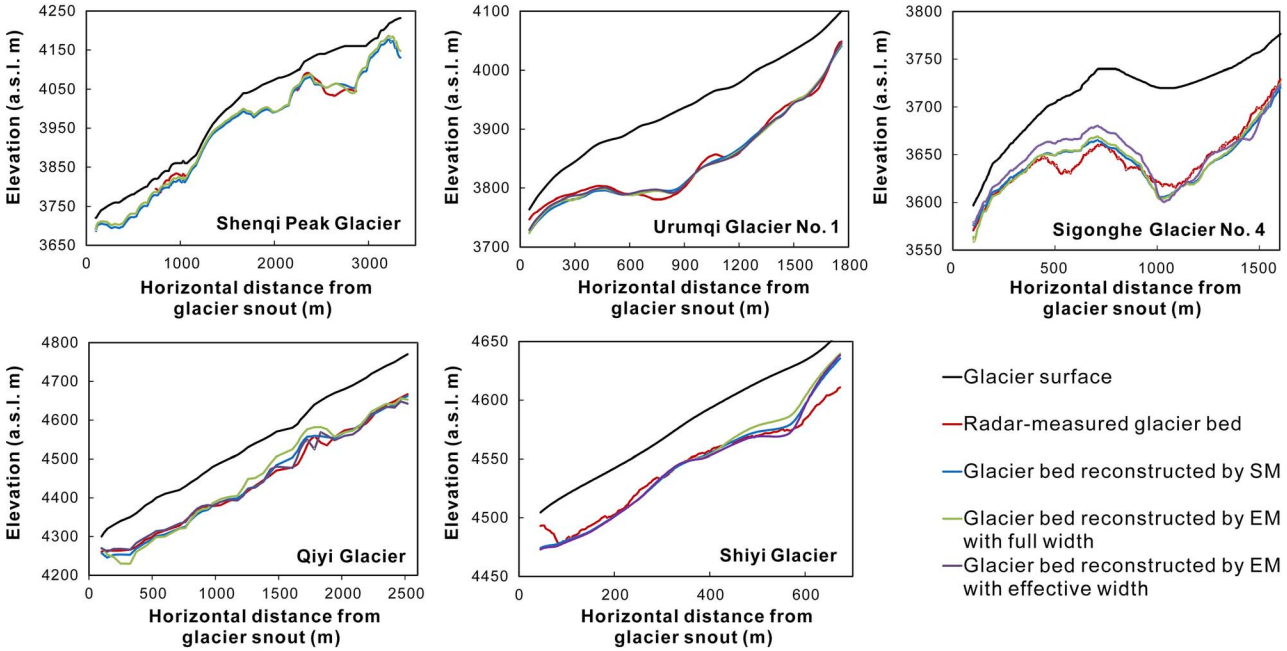

Figure 3. Bed profiles along the flow line of each of our five glaciers reconstructed by our three methods of ice-thickness estimation: standard method (SM), extended method (EM) using full width, and extended method using effective width. Also shown for each glacier are its known surface topography (in black) and radar-measured bed profile (in red).

three methods thus seem to be successful, despite our having assumed a constant yield stress for each glacier. However, Table 3 shows that the optimal values of τ_y vary across methods and glaciers over a vast range (50–175 kPa). Variation of τ_y for each method is less, but still spans a factor of 2 to 3.

[25] A clear pattern in Table 3 is that, for each glacier, the optimal value of τ_y in the standard method is higher than that in both extended methods. This is expected because the latter methods account for the effect of side drag, which takes up part of the driving stress (section 2.2). τ_y in the EM-FW is also higher than that in the EM-EW, consistent with *Nye*'s [1965] result that a narrower glacier cross section has a smaller shape factor f (Figure 1).

[26] The range in τ_y inferred here raises uncertainty regarding its choice when the methods are applied genuinely to glaciers that lack any thickness data; however, the impact of such uncertainty can be gauged using sensitivity analysis, which we do in section 4.2. Still, it is encouraging for us to find that for a given glacier, a single τ_y value suffices for producing thickness estimates that closely follow variations in the observed thickness along the flow line (Figure 4). Not only does this result lend support to the perfect-plasticity formulation; it suggests also that τ_y for each glacier

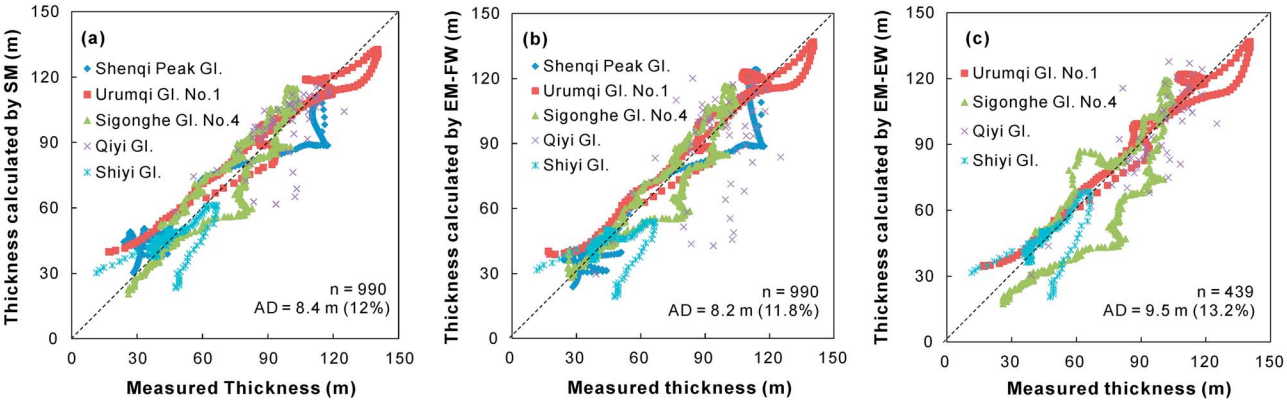

Figure 4. Comparison of measured ice thicknesses and the ice thicknesses estimated by three methods: (a) SM, (b) extended method using full width (EM-FW), and (c) extended method using effective width (EM-EW). Shenqi Peak Glacier is omitted from Figure 4c because its EM-EW results are the same as those for EM-FW, as explained in the text (n, number of points of comparison; AD, average deviation.)

Table 4. Average Deviation Between Measured and Estimated Ice Thicknesses When Each of Our Three Thickness-Estimation Methods is Applied to Each Glacier[a]

				Qiyi Glacier		
	Shenqi Peak Glacier	Urumqi Glacier No. 1	Sigonghe Glacier No. 4	Whole	Tongue	Shiyi Glacier
n	251	162	371	48	28	158
Length (m)	1000	1710	1540	2420	1380	630
Average deviation for SM (m)	12.8 (26.3%)	7.4 (7.9%)	7.7 (10.9%)	10.1 (10.6%)	8.3 (9.2%)	5.4 (11.7%)
Average deviation for EM-FW (m)	9.4 (19.2%)	6.6 (7.1%)	7.7 (10.8%)	19.0 (18.2%)	4.8 (5.3%)	7.8 (16.8%)
Average deviation for EM-EW (m)	9.4 (19.2%)	5.8 (6.2%)	13.2 (18.6%)	9.3 (9.7%)	4.8 (5.3%)	6.0 (12.8%)

[a]Application of each method assumes $\alpha_0 = 4°$, $\alpha_{lim} = 30°$, and the optimal values of τ_y in Table 3. "Length" refers to the total distance of radar lines on the glacier, and *n* refers to the total number of points where measured and estimated ice thicknesses are compared. For the average deviation rows, the values in parentheses express the average deviation as a percentage of each glacier's mean measured flow line thickness. SM, standard method; EM-FW, extended method using full width; EM-EW, extended method using effective width.

may be constrained reasonably by just a few ice-thickness measurements.

4. Discussion

4.1. Evaluating the Methods' Performance

[27] In physical terms, the extended methods are more realistic than the standard method because they account for side drag on the glaciers. Thus their optimized τ_y values may be considered as truer reflections of basal resistance, which is mostly controlled by the material and temperature, not the topography of individual glaciers, giving the potential to use the constant yield stress in a region with similar climate regime. But do the extended methods deliver more accurate ice thicknesses than the standard method? We assess this by examining Table 4, which lists the average deviations (between estimated and measured ice thicknesses) from using each method on each glacier. The variations in Table 4 stem partly from the differing geometry of our glaciers, and interpreting them helps us understand our extended methods' limitations. To aid our evaluation, we add a column in Table 4 for Qiyi Glacier that shows the average deviations for its lower tongue only.

[28] We reported above that the methods do not differ much in how well they reproduce the thickness variances of all five glaciers. At first glance, the results in Table 4 support this observation. While the extended methods (EM-FW, EM-EW) deliver average deviation that are sometimes lower than that for the standard method (SM), sometimes their average deviations are higher, and much worse in the case of Sigonghe Glacier No. 4 with EM-EW. For the three methods SM, EM-FW and EM-EW, average deviations averaged over all five glaciers are 8.4 m (12.0%), 8.2 m (11.8%) and 9.5 m (13.2%), respectively. We show below, however, that the latter two methods, notably EM-EW, can excel in certain situations.

[29] First, Table 4 indicates success for the extended methods over the standard one for Shenqi Peak Glacier, Urumqi Glacier No. 1 and the lower tongue of Qiyi Glacier (in achieving low average deviations); the respective good matches between estimated and measured bed profiles can be seen in Figure 3. Thus, accounting for the glacier width is apparently crucial for getting the ice thickness right for these study sites. We notice two things in common about these sites: (1) their ice flows are well constrained by valley topography, allowing us to estimate the full widths and effective widths of cross sections straightforwardly, and (2) these width estimates were identical or similar (Figure 2). Steep sidewalls confine the lower tongues of Shenqi Peak Glacier and Qiyi Glacier where our thickness comparisons are made. Urumqi Glacier No. 1 is a cirque glacier without an elongated lower tongue, but has steep walls on the sides. On this glacier, the extended methods do not reduce the average deviation as much as it did for Qiyi Glacier, but yield low average deviations that are only 6–7% of the mean flow line thickness.

[30] These results suggest that our extended method (meaning both EM-FW and EM-EW) can yield reliable thickness estimates when there is little ambiguity in the choice of the glacier width. A key example is the lower tongue of Qiyi Glacier, where it vastly improves upon the standard method, reducing its average deviation by almost a factor of 2. In this regard, Figure 5 shows that cross-sectional profiles of the bed reconstructed by EM-FW and EM-EW on this tongue provide reasonable match to the measured bed positions. In this example, the two extended methods yield identical results because the full and effective widths on the tongue are equal. Also, although the methods predict parabolic and therefore symmetric cross profiles of ice thickness, the reconstructed bed profiles in Figure 5 are asymmetric because they have been calculated by subtracting the ice thickness from the known glacier surface elevation, whose cross profiles are not symmetric.

[31] The other results for Qiyi Glacier show what could happen if the width is misjudged. In contrast to what we just described for its lower tongue, column 5 in Table 4 shows that for the whole glacier, EM-FW performs much worse than the standard method. The reason for this may be diagnosed from Figure 2, which shows that full widths constructed for the upper part of this glacier differ substantially from the effective widths. Ridges divide the glacier here into three catchments, which are not resolved by the full widths; consequently, the widths used in the EM-FW are overestimates, and they bias its yield stress and thickness results. Furthermore, Table 4 shows that for the whole glacier, EM-EW performs better than EM-FW, but improves on the standard method only slightly; this means that using a threshold slope to define the effective width alleviates the problem, but by no means resolves it. These results show that our simple procedure in section 2.3 of deriving the width from geometric information alone (glacier outline and topography) may not suffice for some glaciers. To obtain

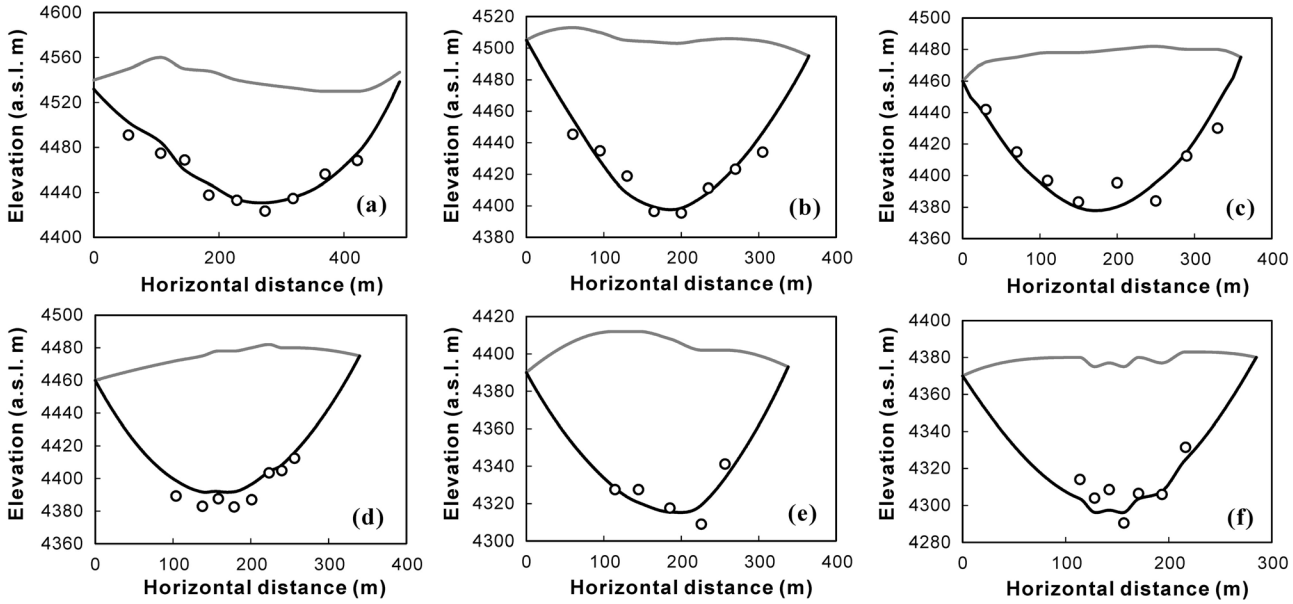

Figure 5. Comparison of transverse glacier-bed profiles reconstructed by our extended methods EM-FW and EM-EW (black curves) against radar-measured bed elevations (circles) at six cross sections on the lower tongue of Qiyi Glacier, located at (a) 1188 m, (b) 1037 m, (c) 897 m, (d) 645 m, (e) 483 m, and (f) 317 m upstream from the snout. Grey curves plot known glacier surface elevations.

reliable width input for the extended methods, it may be necessary to study the glacier's surface-velocity pattern (if maps of this are available) or geomorphic features (e.g., moraines and crevasses) through remote-sensing images or field observations.

[32] Shiyi Glacier is another example where improper estimation of glacier width leads to poorer results in the extended methods than in the standard method. This glacier splits into two branches, and this causes the full widths drawn for the upper glacier to overestimate the width of its western main branch (Figure 2). EM-EW improves on EM-FW also in this case, but does not out perform the standard method. We learn from this glacier and Qiyi Glacier that inaccurate width assignment in the extended methods could bias their optimal yield stress so much that they perform worse than the standard method, even though the latter method does not account for side drag at all.

[33] Last we consider Sigonghe Glacier No. 4, whose flow is constrained by steep sidewalls for most of its length. On the basis of this and our previous discussion, we expect the extended methods to do well on this glacier, but this is not the case. EM-EW delivers the worst results of all three methods, while EM-FW only matches the standard method's performance. Figure 3 shows that ice thickness reconstructed by the extended methods for this glacier reproduces measured thickness poorly on its lower part (notably in the area ~400–500 m up glacier from the snout). The ice surface here is gentle with slope angles near 0° at many places, and our detailed analysis of the errors shows that most of them arise from our use of the minimum slope limit ($\alpha_0 = 4°$, section 2) in this area. Our field observations also confirm that the effective widths do not delineate actual widths correctly on the upper part of the glacier, where a prominent tributary joins it from the east. In this example of Sigonghe Glacier No. 4, we see the extended methods compromised by inaccuracies in multiple input parameters.

[34] Despite our relatively small data set of five glaciers, we can summarize with some general recommendations for the extended method. This method can give superior results compared to the standard method but requires accurate input parameters, notably the glacier width. Mountain glaciers are often fed by separate tributaries, and some have lower tongues that split around bed obstacles. Careful prescription of the half width w is important in these cases. We expect the method to work well for cross sections constrained strongly by sidewalls, for example, long narrow trunks, or higher-order tributaries with these characteristics. For other cross sections, we caution against the use of the purely geometry-based procedure in section 2.3 to determine the width, which may be grossly inaccurate; and we suggest cross-checking with independent (field- or remote-sensing based) information wherever possible in such determination. This caveat must be borne in mind when applying the method to large samples of glaciers, where a paucity of such information is likely.

4.2. Sensitivity Analysis

[35] Finally, we study to what extent uncertainties in the inputs of the extended method influence its thickness estimates, by conducting sensitivity tests where each input (yield stress τ_y, surface slope α, glacier half width w) is altered by a small amount in turn. Through this section, we define "sensitivity" (Δh) as the resulting change in the estimated ice thickness divided by its unperturbed value, expressed as a percentage. For our five glaciers, the unperturbed value is each glacier's mean estimated ice thickness found from Figure 3. The results reported below are useful for gauging potential errors in the ice thickness, which propagate into

Table 5. Sensitivity of the Ice Thickness (Δh) Estimated by Our Extended Methods (EM-FW and EM-EW) to Changes in the Input Parameters of Yield Stress τ_y, Surface Slope α, and Half Width w When the Methods Are Used on Five Glaciers in Northwest China[a]

	Shenqi Peak Glacier	Urumqi Glacier No. 1		Sigonghe Glacier No. 4		Qiyi Glacier		Shiyi Glacier	
		EM-FW	EM-EW	EM-FW	EM-EW	EM-FW	EM-EW	EM-FW	EM-EW
$\Delta\tau_y = +10\%$	+13.1	+14.1	+15.5	+12.2	+14.6	+8.2	+26.6	+12.5	+13.5
$\Delta\alpha = +1°$	−15.4	−11.7	−12.7	−14.4	−16.1	−5.2	−17.6	−8.1	−8.8
$\Delta w = +10\%$	−2.4	−3.1	−4.1	−1.7	−3.1	−5.0	−5.1	−1.9	−2.7

[a]The sensitivity (Δh) measures the changes in the mean estimated ice thickness divided by its unperturbed value, expressed as a percentage. Only one column of results is shown for Shenqi Peak Glacier, because these results are the same for EM-FW and EM-EW.

quantities based subsequently on it (e.g., glacier volumes). They are relevant especially because the yield stress τ_y is not observable and could only be found by calibration (e.g., section 3.2) or inferred indirectly from other glaciers. Parameters of this kind appear in other methods of thickness estimation, where sensitivity analyses have been used to quantify their impact.

[36] Table 5 presents the results for our five glaciers and for our two versions of the extended method employing the full width (FW) and the effective width (EW). The estimated thickness depends most sensitively on τ_y and α. Generally, a 10% change in τ_y or 1° change in α causes changes in Δh by 10 to 20%. In absolute terms (and on average), an increase of 10 kPa in τ_y raises the thickness by 14.4%, whereas a 1° increase in α lowers the thickness by 12.2%, so a reduction in α by 1.2° could offset the former change. By comparison, the thickness is less sensitive to changes in the half width: raising w by 10% reduces the thickness by only 3.2% on average.

[37] A more general sensitivity analysis can be made by differentiating h in equation (6) (where $H = \tau_y/\rho g \sin\alpha$) with respect to each input. We do this here for the two most sensitive inputs (yield stress τ_y and surface slope α) in order to calculate $(\partial h/\partial\alpha)/h$ and $(\partial h/\partial\tau_y)/h$, which are in equivalent terms as our sensitivity measure Δh. Both $(\partial h/\partial\alpha)/h$ and $(\partial h/\partial\tau_y)/h$ are functions of τ_y, α, and w. However, for the purpose of illustration, here we set the half width w (the least sensitive parameter) to a constant 500 m, which is of the size order typical for glaciers in northwest China [*Wang et al.*, 1981; *Liu et al.*, 1982; *Wang et al.*, 1987].

[38] Figure 6 plots $(\partial h/\partial\alpha)/h$ for an input perturbation of $\Delta\alpha = +1°$. We see that sensitivity of the thickness to changes in surface slope is always negative (steepening thins the ice), and diminishes as the slope increases. In other words, thickness estimates made for shallower glaciers are more sensitive to errors in the slope. This sensitivity (to changes in slope) increases with the yield stress, but, as shown by the two curves in Figure 6, is only weakly dependent on it over the range of optimal yield stresses for our five glaciers (Table 3). For these glaciers, which have surface slopes of around 10 to 20°, this sensitivity ranges between −4% to −11%.

[39] Figure 7 plots $(\partial h/\partial\tau_y)/h$ for an input perturbation of $\Delta\tau_y$ = +10 kPa. Sensitivity of the estimated thickness to changes in the yield stress is always positive; thus, as equation (6) predicts, the extended method (like the standard method) reconstructs thicker ice when τ_y is greater. However, this sensitivity diminishes with τ_y, meaning that thickness estimates made for glaciers with lower yield stress are more sensitive to uncertainty in this input.

5. Conclusions and Outlook

[40] We have developed a new method, based on the perfect-plastic rheology assumption, for estimating the flow

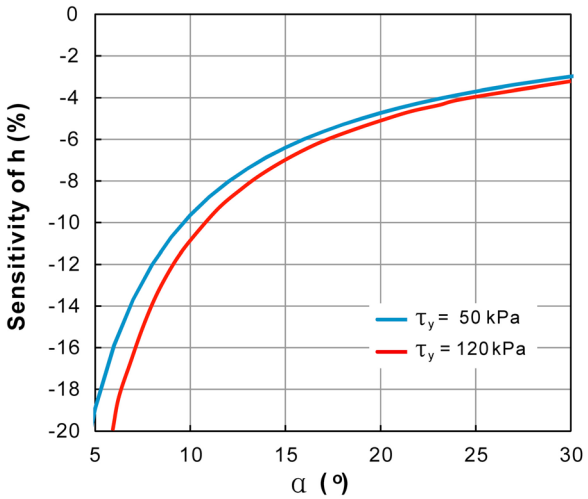

Figure 6. Sensitivity of the ice-thickness estimate produced by our extended method for a 1° increase in the input surface slope.

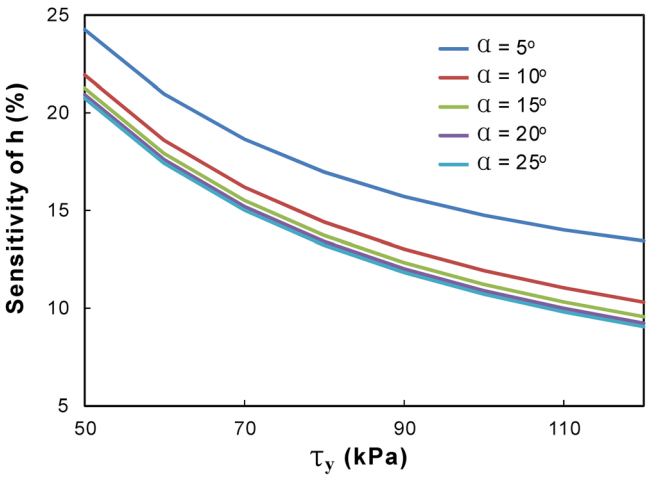

Figure 7. Sensitivity of the ice-thickness estimate produced by our extended method for a 10 kPa increase in the input yield stress.

line thickness of glaciers from their observable surface parameters. The method accounts for the cross-sectional width of the flow and requires glacier geometry data and an assumed yield stress as inputs. Its validation against data from five glaciers demonstrates its potential to give useful thickness estimates. When the yield stress is chosen to optimize the match in thickness, these estimates fall within 11.8% of the actual thicknesses (a result that lumps the average deviations in Table 4 for EM-FW and EM-EW), meaning that they can reproduce well the variations of glacier thickness along flow lines. A novelty of the method is its inclusion of side drag in the force-balance calculation; thus it requires accurate determination of the width of each cross section from observations. Compared with most other existing methods, its key advantage is simplicity: its inputs are few and straightforward to derive, and its physical basis is easy to understand. More sophisticated methods typically require data for glacier mass balance or surface velocity, and these are challenging to obtain for many glaciers.

[41] Uncertainty surrounds the choice of the yield stress τ_y when our method is applied to glaciers where independent ice-thickness data are lacking. Nevertheless, our sensitivity analysis (section 4.2) along with the typical expected range of τ_y (we found 50 to 175 kPa for our glaciers) can help to constrain errors in the thickness estimates. Since this yield stress τ_y ultimately parameterizes a glacier's basal resistance, however complex are the physics behind this, there may exist statistical links between τ_y and environmental and climatic factors for large populations of glaciers. Even if such links turn out to be weak, the statistical properties of τ_y can help us quantify the reliability of the method. For these reasons, future research should seek abundant data on τ_y for different glaciers (such data are severely lacking at present), an effort that will also inform studies that use the perfect-plasticity approach to reconstruct paleoglaciers [*Schilling and Hollin*, 1981; *Benn and Hulton*, 2010; *Ng et al.*, 2010].

[42] In this paper, we have focused on the theoretical underpinnings of the method and tested it with only a handful of glaciers. A natural next step is to assess its applicability for glaciers on a regional scale (the Tian Shan and Qilian Shan being candidates) and estimate their thicknesses and volumes. At the same time, it is desirable to compare the performance of the spectrum of methods and identify preferred methods for specific situations. A useful comparison is that between simple methods (like ours) and sophisticated methods. One hypothesis is that the latter methods might yield superior results because they contain more detailed physics. On the other hand, since their greater number of input parameters necessitate more tuning, for large glacier populations their success may depend more critically on the availability of observable parameter constraints than in simple methods. These considerations suggest that a versatile solution to the problem of glacier-thickness estimation may rest on combining different methods to cope with the diversity of glacier types and available information.

[43] **Acknowledgments.** We thank A. Densmore and B. Hubbard (Editors) and three anonymous reviewers for their constructive comments and criticism on the paper. This research was supported by the National Basic Research Program of China (2010CB951003), the Knowledge Innovation Project of the Chinese Academy of Sciences (KZCX2-EW-311), and the National Natural Science Foundation of China (91025012, 41101066, 40930526, and J0930003/J0109).

References

Aðalgeirsdóttir, G., T. Jóhannesson, H. Björnsson, F. Pálsson, and O. Sigurðsson (2006), Response of Hofsjökull and southern Vatnajökull, Iceland, to climate change, *J. Geophys. Res.*, *111*, F03001, doi:10.1029/2005JF000388.

Aniya, M., and R. Welch (1981), Morphological analyses of glacial valleys and estimates of sediment thickness on the valley floor: Victoria Valley system, Antarctica, *Antarct. Rec.*, *71*, 76–95.

Arendt, A., K. Echelmeyer, W. Harrison, C. Lingle, S. Zirnheld, V. Valentine, B. Ritchie, and M. Druckenmiller (2006), Updated estimates of glacier volume changes in the western Chugach Mountains, Alaska, and a comparison of regional extrapolation methods, *J. Geophys. Res.*, *111*, F03019, doi:10.1029/2005JF000436.

Bahr, D. B., M. F. Meier, and S. D. Peckham (1997), The physical basis of glacier volume-area scaling, *J. Geophys. Res.*, *102*, 20,355–20,362, doi:10.1029/97JB01696.

Beget, J. (1987), Low profile of the northwest Laurentide Ice Sheet, *Arct. Alp. Res.*, *19*(1), 81–88, doi:10.2307/1551003.

Benn, D. I., and N. R. J. Hulton (2010), An Excel™ spreadsheet program for reconstructing the surface profile of former mountain glaciers and ice caps, *Comput. Geosci.*, *36*(5), 605–610, doi:10.1016/j.cageo.2009.09.016.

Björnsson, H., G. Aðalgeirsdóttir, S. Guðmundsson, T. Jóhannesson, O. Sigurðsson, and F. Pálsson (2006), Climate change response of Vatnajökull, Hofsjökull and Langjökull ice caps, Iceland, paper presented at European Conference on Impacts of Climate Change on Renewable Energy Sources, Natl. Energy Serv., Reykjavik, 5–9 June. [Available at http://www.raunvis.hi.is/~sg/bjornsson_et_al.pdf.]

Budd, W. F. (1969), The dynamics of ice masses, *Sci. Rep. 108*, Aust. Natl. Antarct. Res. Exped., Melbourne, Victoria.

Cao, M., Z. Li, and H. Li (2011), Features of the surface flow velocity on the Qingbingtan Glacier No. 72, Tianshan Mountains [in Chinese with English abstract], *J. Glaciol. Geocryol.*, *33*(1), 21–29.

Chen, J., and A. Ohmura (1990), Estimation of Alpine glacier water resources and their change since the 1870s, *IAHS Publ.*, *193*, 127–135.

Clarke, G. K. C., E. Berthier, C. G. Schoof, and A. H. Jarosch (2009), Neural networks applied to estimating subglacial topography and glacier volume, *J. Clim.*, *22*(8), 2146–2160, doi:10.1175/2008JCLI2572.1.

Doornkamp, J. C., and C. A. M. King (1971), *Numerical Analysis in Geomorphology: An Introduction*, Edward Arnold, London.

Driedger, C. L., and P. M. Kennard (1986), Glacier volume estimation on Cascade volcanoes: An analysis and comparison with other methods, *Ann. Glaciol.*, *8*, 59–64.

Farinotti, D., M. Huss, A. Bauder, M. Funk, and M. Truffer (2009), A method to estimate the ice volume and ice-thickness distribution of alpine glaciers, *J. Glaciol.*, *55*(191), 422–430, doi:10.3189/002214309788816759.

Gerrard, J. A. F., M. F. Perutz, and A. Roch (1952), Measurement of the velocity distribution along a vertical line through a glacier, *Proc. R. Soc. London, Ser. A*, *213*(1115), 546–558, doi:10.1098/rspa.1952.0144.

Graf, W. L. (1970), The geomorphology of the glacial valley cross section, *Arct. Alp. Res.*, *2*(4), 303–312, doi:10.2307/1550243.

Haeberli, W., and M. Hoelzle (1995), Application of inventory data for estimating characteristics of and regional climate-change effects on mountain glaciers: A pilot study with the European Alps, *Ann. Glaciol.*, *21*, 206–212.

Harbor, J. (1990), A discussion of Hirano and Aniya's (1988, 1989) explanation of glacial-valley cross profile development, *Earth Surf. Processes Landforms*, *15*(4), 369–377, doi:10.1002/esp.3290150408.

Harbor, J. M., and D. A. Wheeler (1992), On the mathematical description of glaciated valley cross sections, *Earth Surf. Processes Landforms*, *17*(5), 477–485, doi:10.1002/esp.3290170507.

Hirano, M., and M. Aniya (1988), A rational explanation of cross-profile morphology for glacial valleys and of glacial valley development, *Earth Surf. Processes Landforms*, *13*(8), 707–716, doi:10.1002/esp.3290130805.

Hubbard, A., H. Blatter, P. Nienow, D. Mair, and B. Hubbard (1998), Comparison of a three-dimensional model for glacier flow with field data from Haut Glacier d'Arolla, Switzerland, *J. Glaciol.*, *44*(147), 368–378.

Huss, M., D. Farinotti, A. Bauder, and M. Funk (2008), Modelling runoff from highly glacierized alpine drainage basins in a changing climate, *Hydrol. Processes*, *22*(19), 3888–3902, doi:10.1002/hyp.7055.

Huybrechts, P., and J. de Wolde (1999), The dynamic response of the Greenland and Antarctic Ice Sheets to multiple-century climatic warming, *J. Clim.*, *12*(8), 2169–2188, doi:10.1175/1520-0442(1999)012<2169:TDROTG>2.0.CO;2.

Huybrechts, P., P. de Nooze, and H. Decleir (1989), Numerical modeling of Glacier d'Argentiere and its historic front variations, in *Glacier*

Fluctuations and Climate Change, edited by J. Oerlemans, pp. 373–398, Kluwer Acad., Dordrecht, Netherlands.

Kamb, B., and K. A. Echelmeyer (1986), Stress-gradient coupling in glacier flow: I. Longitudinal averaging of the influence of ice thickness and surface slope, *J. Glaciol.*, *32*(111), 267–284.

Kaser, G., M. Großhauser, and B. Marzeion (2010), Contribution potential of glaciers to water availability in different climate regimes, *Proc. Natl. Acad. Sci. U. S. A.*, *107*(47), 20,223–20,227, doi:10.1073/pnas.1008162107.

Lemke, P., et al. (2007), Observations: Changes in snow, ice and frozen ground, in *Climate Change 2007: The Physical Science Basis. Contribution of Working Group I to the Fourth Assessment Report of the Intergovernmental Panel on Climate Change*, edited by S. Solomon et al., pp. 337–383, Cambridge Univ. Press, Cambridge, U. K.

Li, Y., G. Liu, and Z. Cui (2001), Glacial valley cross-profile morphology, Tian Shan Mountains, China, *Geomorphology*, *38*, 153–166, doi:10.1016/S0169-555X(00)00078-7.

Li, Z., K. Li, and L. Wang (2010), Study on recent glacier changes and their impact on water resources in Xinjiang, North Western China [in Chinese with English abstract], *Quat. Sci.*, *30*(1), 96–106.

Liu, C., et al. (1982), *Glacier Inventory of China*, vol. 2, *Altai Mountains*, China Sci. Press, Beijing.

Ng, F., I. D. Barr, and C. D. Clark (2010), Using the surface profiles of modern ice masses to inform palaeo-glacier reconstructions, *Quat. Sci. Rev.*, *29*, 3240–3255, doi:10.1016/j.quascirev.2010.06.045.

Nye, J. F. (1951), The flow of glaciers and ice-sheets as a problem in plasticity, *Proc. R. Soc. London, Ser. A*, *207*(1091), 554–572, doi:10.1098/rspa.1951.0140.

Nye, J. F. (1952), The mechanics of glacier flow, *J. Glaciol.*, *2*(12), 82–93.

Nye, J. F. (1965), The flow of a glacier in a channel of rectangular, elliptic or parabolic cross-section, *J. Glaciol.*, *5*(41), 661–690.

Oerlemans, J. (1997), Climate sensitivity of Franz Josef Glacier, New Zealand, as revealed by numerical modeling, *Arct. Alp. Res.*, *29*(2), 233–239, doi:10.2307/1552052.

Oerlemans, J., et al. (1998), Modelling the response of glaciers to climate warming, *Clim. Dyn.*, *14*(4), 267–274, doi:10.1007/s003820050222.

Paterson, W. S. B. (1970a), The sliding velocity of Athabasca Glacier, Canada, *J. Glaciol.*, *9*(55), 55–63.

Paterson, W. S. B. (1970b), The application of ice physics to glacier studies, in *Glaciers: Proceedings of Workshop Seminar, 1970*, pp. 43–46, Can. Natl. Comm. for the Int. Hydrol. Decade, Ottawa.

Paterson, W. S. B. (1994), *The Physics of Glaciers*, 3rd ed., 480 pp., Elsevier Sci., New York.

Paul, F., and F. Svoboda (2010), A new glacier inventory on southern Baffin Island, Canada, from ASTER data: II. Data analysis, glacier change and applications, *Ann. Glaciol.*, *50*, 22–31, doi:10.3189/172756410790595921.

Radic, V., and R. Hock (2010), Regional and global volumes of glaciers derived from statistical upscaling of glacier inventory data, *J. Geophys. Res.*, *115*, F01010, doi:10.1029/2009JF001373.

Raper, S. C. B., and R. J. Braithwaite (2006), Low sea level rise projections from mountain glaciers and icecaps under global warming, *Nature*, *439*, 311–313, doi:10.1038/nature04448.

Raymond, M. J., and G. H. Gudmundsson (2009), Estimating basal properties of ice streams from surface measurements: A non-linear Bayesian inverse approach applied to synthetic data, *Cryosphere*, *3*, 265–278, doi:10.5194/tc-3-265-2009.

Reeh, N. (1982), A plasticity theory approach to the steady-state shape of a three-dimensional ice sheet, *J. Glaciol.*, *28*(100), 431–455.

Reeh, N. (1984), Reconstruction of the glacial ice covers of Greenland and the Canadian Arctic Islands by three-dimensional, perfectly plastic ice-sheet modelling, *Ann. Glaciol.*, *5*, 115–121.

Schilling, D. H., and J. T. Hollin (1981), Numerical reconstructions of valley glaciers and small ice caps, in *The Last Great Ice Sheets*, edited by G. H. Denton and T. J. Hughes, pp. 207–220, John Wiley, New York.

Shi, Y., Y. Shen, E. Kang, D. Li, Y. Ding, G. Zhang, and R. Hu (2006), Recent and future climate change in Northwest China, *Clim. Change*, *80*(3–4), 379–393.

Shi, Y., M. Huang, T. Yao, and Y. He (Eds.) (2008a), *Glaciers and Related Environments in China*, China Sci. Press, Beijing.

Shi, Y., S. Liu, B. Ye, C. Liu, and Z. Wang (2008b), *Concise Glacier Inventory of China*, Shanghai Pop. Sci. Press, Shanghai, China.

Svensson, H. (1959), Is the cross-section of a glacial valley a parabola?, *J. Glaciol.*, *3*(25), 362–363.

Thorsteinsson, T., C. F. Raymond, G. H. Gudmundsson, R. A. Bindschadler, P. Vornberger, and I. Joughin (2003), Bed topography and lubrication inferred from surface measurements on fast-flowing ice streams, *J. Glaciol.*, *49*(167), 481–490, doi:10.3189/172756503781830502.

Van de Wal, R. S. W., and M. Wild (2001), Modelling the response of glaciers to climate change by applying volume-area scaling in combination with a high resolution GCM, *Clim. Dyn.*, *18*(3–4), 359–366, doi:10.1007/s003820100184.

Wang, P., Z. Li, and H. Li (2011), Ice volume changes and their characteristics for representative glacier against the background of climatic warming: A case study of Urumqi Glacier No. 1, Tianshan, China [in Chinese with English abstract], *J. Nat. Resour.*, *26*(7), 1189–1198.

Wang, Y., et al. (1981), *Glacier Inventory of China*, vol. 1, *Tianshan Mountains*, China Sci. Press, Beijing.

Wang, Z., et al. (1987), *Glacier Inventory of China*, vol. 3, *Qilian Mountains*, China Sci. Press, Beijing.

Wu, L., Z. Li, P. Wang, H. Li, and F. Wang (2011), Sounding the Sigong River Glacier No. 4 in Mt. Bogda area, the Tianshan Mountains by using ground penetrating radar and estimating the ice volume [in Chinese with English abstract], *J. Glaciol. Geocryol.*, *33*(2), 276–282.

Zhou, Z., Z. Li, H. Li, and Z. Jing (2009), The flow velocity features and dynamic simulation of the Glacier No. 1 at the headwaters of Urumqi River, Tianshan Mountains [in Chinese with English abstract], *J. Glaciol. Geocryol.*, *31*(1), 55–61.

G. Cheng, H. Li, Z. Li, and D. Qin, State Key Laboratory of Cryospheric Sciences, Tian Shan Glaciological Station, CAREERI, CAS, Lanzhou 730000, China. (lizq@lzb.ac.cn)

F. Ng, Department of Geography, University of Sheffield, Sheffield S10 2TN, UK.